A Simple procedure to evaluate the efficiency and power density of power conversion topologies for offshore wind turbines

Rene Barrera-Cardenas[a,*], Marta Molinas[a]

[a]Department of Electric Power Engineering, Norwegian University of Science and Technology, NO-7491, Trondheim, Norway

Abstract

The prospective development of the offshore wind energy conversion system is mainly promoted by demand for higher efficiency and power density. This paper describes a simple procedure to calculate the efficiency and power density of power conversion systems for offshore wind turbines. The proposed method can be used as starting point into the linear design process to calculate the losses in semiconductors and transformer as well as the volume of main elements. With the losses and volumes, efficiency and power density can be calculated. In order to illustrate the evaluation procedure, the reduced matrix converter with single-phase transformer is considered like example topology. The Efficiency-Power-density Pareto Front is obtained for a set of design parameters. The methodology is eminently suitable for comparison of power converter with different topologies.

Keywords: WEC system, efficiency, power density, transformer design, offshore power conversion

1. Introduction

One of most important technological challenges related to the optimization of offshore wind energy conversion systems (WEC) is achieve demand for higher efficiency and power density, these performances indices are two conflicting objectives. Requirements of high power density imply compact solutions. Here, medium/high frequency transformers can play an important role since an increase on operation frequency allows for a reduction in the volume of transformer. However, higher frequencies in the power electronic components will generate higher switching losses and therefore deteriorate the efficiency of the system. [1]

During the design of a WEC system one has to determine values of the free design parameters (e.g. circuit elements, switching frequency, turn ratio of transformer) so that the design constraints (e.g. temperature rise, saturation flux density of magnetic materials) are met for the given specifications (e.g. input voltage, power output). In order to find the values of the free design parameters which lead to an optimal design, with respect to the given design objective (maximal efficiency, maximal power density, minimum costs), one needs an automatic optimization procedure [2]. That optimization procedure is based on complete model of

---
*Corresponding author

Email addresses: rene.barrera@elkraft.ntnu.no (Rene Barrera-Cardenas), marta.molinas@ntnu.no (Marta Molinas)
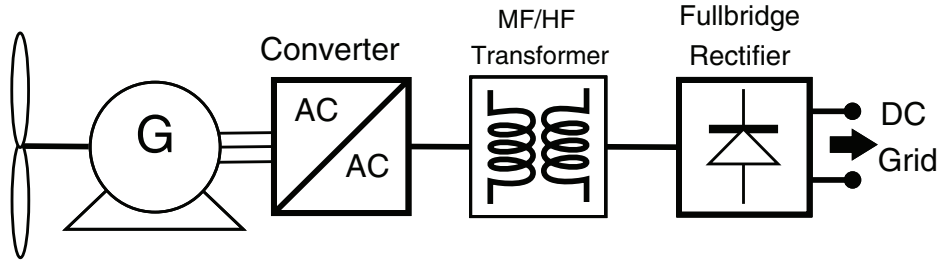
Figure 1: Power conversion scheme for offshore wind turbine

the converter circuit including multi-domain component models. This model could be based on analytical equations, on numerical simulations or on a combination of both. Also, a way to calculate the performance indices of the design objective based on design variables must be defined.

This paper describes a simple procedure to calculate the efficiency and power density of power conversion topologies for offshore wind turbines. The system scheme analysed in this paper is shown in Fig. 1. Basically the proposed scheme to be analysed consists of three stages: ac-ac converter, medium or high frequency transformer and ac-dc full-bridge rectifier. In order to simplify the proposed procedure only the first two stages are considered for this study since these stages are the largest contributors of loss and volume in this scheme. The proposed method can be used like starting point into the linear design process to calculate the losses in semiconductors and transformer as well as the volume of main elements (transformer, semiconductor heat sink). With the losses and volumes, the efficiency and power density can be calculated, respectively. Finally with those results the Efficiency-Power-density Pareto Front for a subspace of design variables can be obtained. A topology known as Reduced Matrix Converter (RMC) and a single-phase transformer are considered in order to illustrate the evaluation procedure. The Efficiency-Power-density Pareto Front is obtained for a set of design parameters.

2. Efficiency and Power Density Evaluation

The efficiency and power density are the performance indices considered in this study. The efficiency (η) of an electrical system is the ratio of power output (P_{out}) and power input (P_{in}), eq. (1). In WEC systems, the power input is determinate by the wind turbine rated and the power output can be expressed as the difference between power input and the losses of the system (P_{losses}). The power input is a design constraint parameter, and then the efficiency is expressed as function of the power losses. The power losses are mainly determinate by two components of the WEC system: the AC/AC converter and the High frequency transformer. In section 2.1 is depicted the equations used to evaluate the main power losses in the WEC system and therefore calculate the system efficiency.

$$\eta = \frac{P_{out}}{P_{in}} = \frac{P_{in} - P_{losses}}{P_{in}} = 1 - \frac{P_{losses}}{P_{in}} \tag{1}$$

In the other hand, the output power density defined by eq. (2), characterize the degree of compactness of a converter. Since the power output can be expressed as function of the power losses, the power density is calculated by evaluates the volume and power losses of the system. In offshore applications, the volume required for realization at a given rated power is mainly determinate by the inductive and capacitive components. However, an extensive study of the power density should include the semiconductors and cooling system volume. In section 2.2 are presented the main considerations to evaluate the volume in the converter.

$$\rho = \frac{P_{out}}{Volume} = \frac{P_{in} - P_{losses}}{Volume} \tag{2}$$

2.1. Power Losses

The converter and transformer losses are considered in this study to evaluate the efficiency and the power density. The main component of the converter is the semiconductor device (IGBT or RB-IGBT). The converter losses are divided into two parts: conduction and switching. The conduction losses model the thermal effect when the device is on state, this power dissipation can be calculated as the product of the voltage across the device (V_{CE}) and the current the device is conducting (I_C) [3], [4].

$$P_{conduction} = V_{CE} \cdot I_C \tag{3}$$

voltage V_{CE} in an IGBT as well as a RB-IGBT is a quadratic function of the collector current (I_C) [5]

$$V_{CE} = K_{CE1} + K_{CE2} \cdot I_C + K_{CE3} \cdot I_C^2 \tag{4}$$

the parameters K_{CE1}, K_{CE2}, K_{CE3} are calculated using the data sheets for each device. Then, the conduction losses can be expressed like (putting (4) in (3)):

$$P_{conduction} = K_{CE1} \cdot I_C + K_{CE2} \cdot I_C^2 + K_{CE3} \cdot I_C^3 \tag{5}$$

It can be observed from (5) that the conduction losses do not depend of the frequency of operation.

On the other hand, the switching losses are produced by the energy dissipated when the semiconductor change between on-state to off-state or vice versa. A method to evaluate that losses based on the energy dissipated in each event is proposed in [5]. The energy dissipated in the device is calculated with

$$E_{sw} = k_1 \cdot I_C^2 + k_2 \cdot I_C \tag{6}$$

k_1 and k_2 are quadratic functions of the voltage between two terminals of the switching at a switching instant (V_C). The relation between k_1 and k_2 with the voltage (V_C) is as follow:

$$k_j = \alpha_{0,j} + \alpha_{1,j} \cdot V_C + \alpha_{2,j} \cdot V_C^2 \tag{7}$$

the coefficient $\alpha_{i,j}$ (with $i=0,1,2$ and $j=1,2$) differ with the type of commutation (turn on, turn off or reverse recovery). The values of $\alpha_{i,j}$ for a 600V/200A RB-IGBT are reported in [5]. In order to calculate the average switching loss, the integral of each commutation energy (E_{sw}) over a time period and dividing by the time period are computed and added.

$$P_{switching} = \frac{1}{T} \cdot \int_{t_o}^{t_0+T} \left(E_{sw-on} + E_{sw-off} + E_{sw-rr} \right) dt \tag{8}$$

An analysis for the losses in reduce matrix converters is presented in [3]. They conclude that switching losses are a linear function of the switching frequency (f_{sw}) in the converter. A similar analysis can be made for other topologies. The switching losses are expressed as follow:

$$P_{switching} = K_{sw1} \cdot f_{sw} \left(K_{sw2} \cdot I_{C(rms)} + K_{sw3} \cdot I_{C(rms)}^2 \right) \tag{9}$$

K_{sw1}, K_{sw2} and K_{sw3} are function of the topology, modulation strategy, blocking voltage, semiconductor type, mainly.

The transformer losses consist mainly of core and copper losses. The total core loss is a result of three loss mechanisms: hysteresis, eddy current and stray losses. The core losses depend of the material, volume core (V_{core}), working frequency (f), flux density amplitude (B_m) and waveform. Steinmetz equation is often used by evaluate the core losses [6, 7]:

$$P_{core} = K_{core} \cdot V_{core} \cdot f^{\alpha c} \cdot B_m^{\beta c} \tag{10}$$

K_{core}, α_C and β_C are constants which can be established from the manufacturer data sheets. However, the values of K_{core} change with the flux density waveform, according to [8]. The manufacturer's data is

normally measured for sinusoidal excitation, therefore such change in K_{core} must be considered to calculate the core losses in presence of different voltage waveform.

The cooper losses are the sum of ohmic losses of all windings:

$$P_{cu} = \sum_{i=1}^{n_w} Kcu_{(i)} \cdot R_{dc(i)} \cdot I_{(i)}^2 = \sum_{i=1}^{n_w} Kcu_{(i)} \cdot \frac{\rho_{cu} \cdot N_{(i)} \cdot MLT_{(i)}}{A_{w(i)}} \cdot I_{(i)}^2 \tag{11}$$

where n_w is the number of windings, I is the rms current value in each winding, R_{dc} is the dc resistance of the winding, ρ_{cu} is the resistivity of the conductor, MLT is the mean length of a turn in the winding, A_w is the wire conduction area, and Kcu is a eddy current loss factor. In High Frequency transformers, eddy current losses in windings, i.e. the losses due to skin and proximity effects, cannot be ignored. The model for estimate the eddy current loss factor, present in [6] and based on Dowell model[9], is used in this paper:

$$Kcu = k_s \cdot k_x \tag{12}$$

$$\Delta_2 = \frac{d}{\delta} = \frac{1.772 \cdot r_o}{\delta} = 1.772 \cdot \Delta_1$$

$$\delta = \sqrt{\frac{\rho_{cu}}{\pi \cdot \mu_o \cdot f \cdot K_{layer}}}$$

$$k_s = \begin{cases} 1 + \frac{\Delta_1^{4}}{48 + 0.8 \cdot \Delta_1^{4}} & \Delta_1 \leq 1.7 \\ 0.25 + 0.5 \cdot \Delta_1 + \frac{3}{32 \cdot \Delta_1} & \Delta_1 > 1.7 \end{cases} \tag{13}$$

$$k_x = 1 + \frac{5 \cdot p_{layer}^2 - 1}{45} \cdot \Delta_2^4 \tag{14}$$

where δ is the skin depth, p_{layer} is the number of layer of winding, Δ_2 is the ratio of the thickness of a layer of foil d to the skin depth δ, and r_o is the radius of an equivalent round conductor ($d = 0.886 \cdot (2r_o)$). $K_{layer} = b_w/(b_l N_{layer})$ is the layer utilization factor. Where N_{layer} and b_l are the number of turns and width of a filled layer, respectively, and b_w is the width of the core window.

The cooper losses for non-sinusoidal waveform can be derived from eq.11 to eq.14 by expanding the current waveform into Fourier series (with n_{fs} terms):

$$P_{cu} = \sum_{i=1}^{n_w} \sum_{j=1}^{n_{fs}} Kcu_{(i,j)} \cdot R_{dc(i)} \cdot I_{rms(i,j)}^2 \tag{15}$$

Also, the passive Components (EMI filter and DC-Link in some topologies) can be included in the total power losses. The energy loss in the inductor can be modeled as transformer losses. However, the losses in the DC-capacitor losses can be neglected due to the low equivalent series resistance of the often used polyethylene capacitors.

Finally, the total power losses considered in this paper is calculated by add the semiconductor losses (conduction eq.5 and switching eq. 9 losses) and transformers losses (core eq.10 and cooper eq.15 losses):

$$P_{losses} = P_{conduction} + P_{switching} + P_{core} + P_{cu} \tag{16}$$

2.2. Volume

The converter volume is given by the semiconductor switches and by heat sink. The switches volume depend of the IGBT module volume ($Vol_{igbtMod}$), the number of devices per IGBT module (n_{dmod}), the number of devices using to implemented the switch (n_{dsw}), and the number total of switches in the topology (n_{Tsw}).

$$Vol_{switches} = n_{Tsw} \cdot \left(\frac{n_{dsw}}{n_{dmod}}\right) \cdot Vol_{igbtMod} \tag{17}$$

Characteristic	Single-phase	Three-phase
Cross-sectional area of the center leg A_{core}	$6a^2$	$6a^2$
Mean length of a turn MLT	$(14 + 2\pi)\,a$	$(14 + 2\pi)\,a$
Window area per phase W_a	$10a^2$	$10a^2$
Core volume V_{core}	$108a^3$	$276a^3$
Winding volume $V_{winding}$	$(140 + 20\pi)\,a^3$	$(420 + 60\pi)\,a^3$
Total surface area of assembled A_t	$(218 + 28\pi)\,a^2$	$(514 + 84\pi)\,a^2$

Table 1: Geometric characteristic of the transformer design process

(a) Single-phase shell-type [11]   (b) Three-phase shell-type
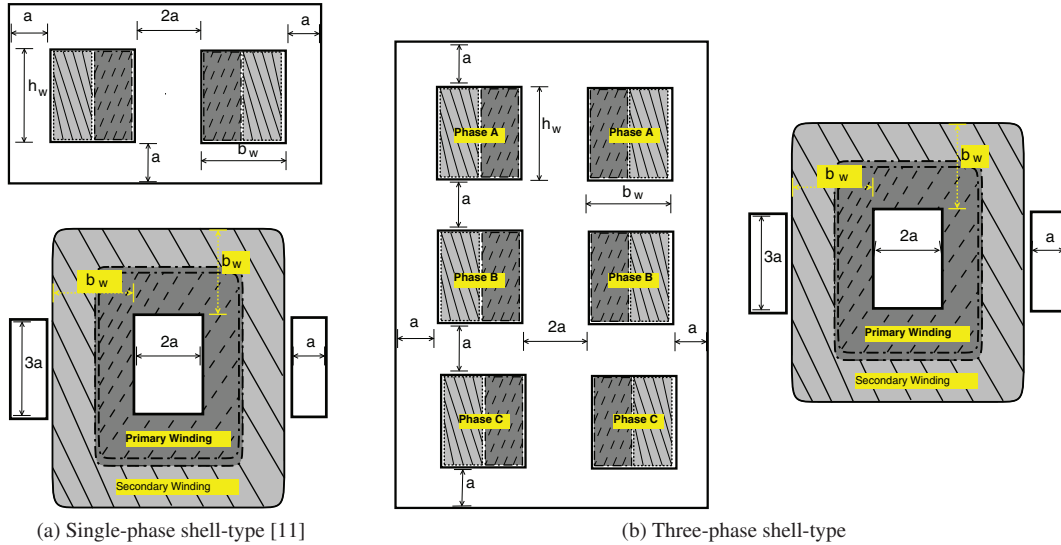
Figure 2: Shell-type transformer Structure

The parameters $Vol_{igbtMod}$ and n_{dmod} can be found in the datasheet of the IGBT module. On the other hand, the heat sink thermal resistance is inversely proportional to the area of heat sink base, then lower thermal resistance requeriments will require more bulky heat sink [10]. Therefore, it is proposed a model of the heat sink volume inversely proportional to the thermal resistance, and combining this model with the definition of thermal resistance is obtained:

$$Vol_{HS} = \frac{K_{HS}}{R_{\theta sa}} = \frac{K_{HS}}{\Delta T_{jamax}/P_{loss}} = \frac{K_{HS}}{\Delta T_{jamax}} \cdot \left(P_{conduction} + P_{switching}\right) \tag{18}$$

where $R_{\theta sa}$ is the thermal resistance, ΔT_{jamax} is the maximum allowable junction-to-ambient temperature, and K_{HS} is a proportionality constant regression found by taking data from different heat sink provided in [10]. In this paper, $\Delta T_{jamax} = 100[K]$ and $K_{HS} = 0.4131[\text{K·dm}^3/\text{W}]$ are the values of the parameters. This approximation of the converter volume may be oversized, but it is practiced when comparing different topologies.

The transformer volume is the result of a process of design, and then there is not expression to directly evaluate the volume. A design process on based a combination of the methods reported in [6], [11] and [7] are used in order to evaluate the transformer volume. Thus design process aims to minimize the volume of the transformer taking into account some assumptions. Such assumptions are described below:

Type transformer structure: the design process is developed for dry shell-type transformers. Fig. 2 shows the front and top section views of the single-phase and three-phase transformers. The relevant core dimensions are indicated on the diagram. The remaining dimensions are adjusted conforming with the recommendation given in [10] ($b_w = 2a$, $h_w = 5a$). Table 1 shows the geometric characteristics define using
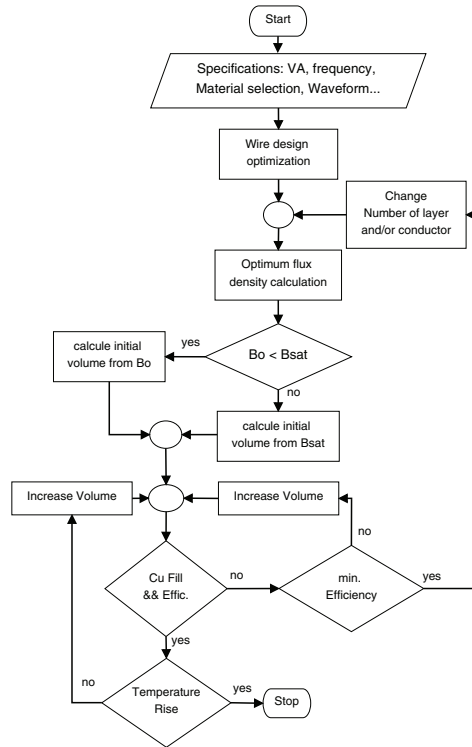
Figure 3: Flowchart of transformer design

this optimal set of relative dimensions the core.

Induced Voltage: the equation for voltage in a transformer winding is given by [6]

$$V_{P(rms)} = K_{wf} \cdot k_f \cdot N_p \cdot f \cdot B_m \cdot A_{core} \tag{19}$$

where K_{wf} is the waveform factor introduced in order to taking into account the ratio of the rms value of the applied voltage waveform, k_f is the core stacking factor (typically is 0.95 for laminated cores), A_{core} is the cross-sectional area of the magnetic core (Table 1), B_m is the flux density amplitude and N_p is the number of turns on the primary. The number of turns on the secondary is given by

$$N_S = \left(\frac{V_S}{V_P} \right) N_P$$

Power rating: An optimum transformer design criterion dictates that the winding power loss on the primary side is equal to that on the secondary side [10, 11]. This criterion implicate that each winding carry the same current density (J). The sum of VA products for each winding of a transformer is of the form [12, 6]:

$$\sum VA = K_{wf} \cdot k_f \cdot \frac{k_b}{K_{cu}} \cdot f \cdot B_m \cdot J \cdot A_{core} \cdot b_w \cdot h_w \tag{20}$$

where k_b is the ratio of bare conductor area to the window area (typically is 0.7), and the other variables as defined above.

Temperature rise: Transformer temperature estimation is needed during the optimization process to verify that temperature specifications are not exceeded. In a transformer with natural air cooling, as considered is this paper, the dominant heat-transfer mechanism is by convection [11]. The Newton's equation of convection is therefore used to determine the temperature rise (ΔT) of the magnetic component [6]:
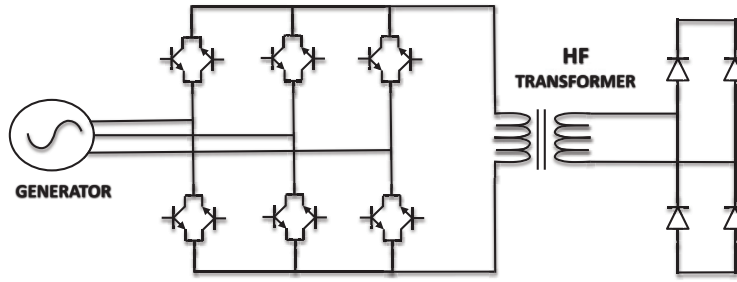
Figure 4: Reduce Matrix Converter and Single-phase Transformer

$$P_{core} + P_{cu} = h_T \cdot A_t \cdot \Delta T \qquad (21)$$

where A_t is the external surface area of the core and windings (Table 1), and h_T is the convection heat-transfer coefficient (typically is 10 W/m².°C [6]).

Optimum flux density criterion: The optimization criterion to minimum losses and the optimum flux density expression presented in [6] had been taken in order to get a first estimation of an optimum volume. That optimum volume is introduced in an iterative process in order to meet the stipulated design requirements and constraints. The flowchart of the minimum transformer volume is shown in Fig. 3. The main constraints considered in this paper are: the maximum allowed temperature rise (ΔT_{max}), the saturation flux density B_{sat}, the copper fill constraint to ensure that the transformer windings fit into the transformer window and the minimum allowed efficiency η_{min}.

Finally, the total volume in this paper is calculated by add the converter volume (switches and heat sink) with the transformer volume (core and windings) obtained from the process described above:

$$Volume = Vol_{switches} + Vol_{HS} + V_{core} + V_{winding} \qquad (22)$$

3. Topology Example

A Reduced Matrix Converter (RMC) with single-phase transformer topology is considered in order to illustrate the efficiency and power density evaluation procedure. The RMC is a direct ac-ac converter with three-phase sinusoidal wave as input and single-phase high frequency square wave as output. This topology is widely studied in [13, 14, 15, 4, 3] and its basic scheme is shown in Fig. 4. The specifications of considered topology are presented in Table 2. A three-phase generator with voltage rms value of 560 [V] is considered as input, and the power rating of the system is 625 [KW]. The RMC is operated like voltage source converter (VSC) and two modulation schemes are regarded: Carrier Base Modulation (CBM) and Space Vector Modulation (SVM). These modulation schemes are presented and analysed by [3] and its characteristics and parameters are taken from the authors report.

The RMC requires bidirectional switches that can be built using two reverse blocking IGBT (RB-IGBTs). This option reduces the number of semiconductors and increases the efficiency compared with using IGBT with anti-parallel diodes for the same purpose[13]. The semiconductor used in this example is a 600V/200A RB-IGBT, and its parameters are reported in [5] and used in [3, 4, 15, 13] to evaluate the converter losses. Four such switches are connected in parallel to have an adequate current rating for the RB-IGBT. For calculating the losses it is assumed that parallel connection does not increase the individual semiconductor loss of the device. Having this assumption, the losses will simply be multiplied by the number of devices and the conducting current divided by the number of devices in parallel.

In this topology, the type of transformer is a single-phase dry shell-type transformer. The voltage input in the transformer is square waveform and its amplitude is approximated to 560 [V] [16]. It is assumed

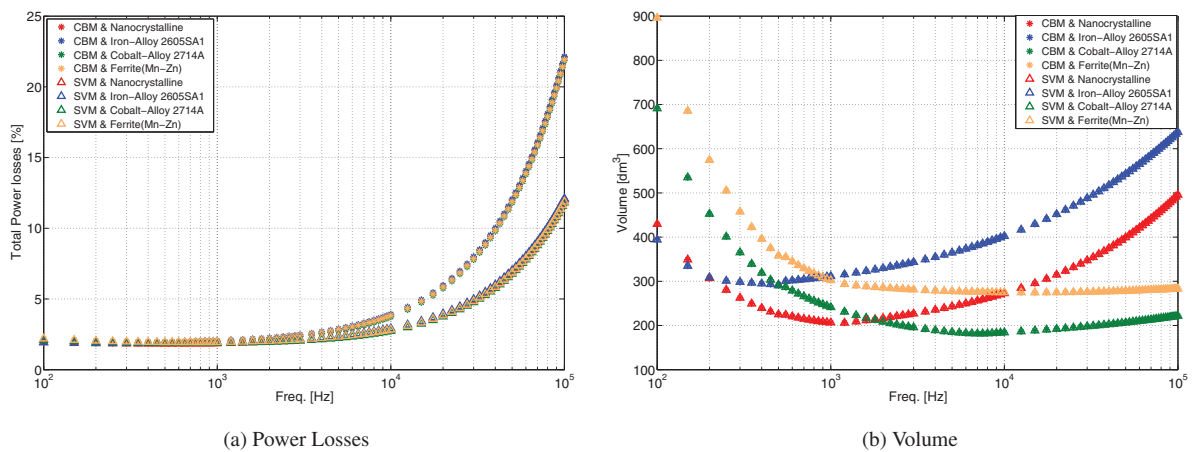| AC-AC Converter	
Topology	Reduced Matrix Converter (RMC)
Operation mode	Voltage source converter (VSC)
Modulation Scheme	Carrier Base Modulation (CBM) and Space Vector Modulation (SVM)
Semiconductor Type	600V/200A RB-IGBT [5]
Voltage waveform	Input: 3-phase sinusoidal wave. Output: 1-phase square wave
High Frequency transformer	
Transformer Type	Single-phase Shell-type
Core Material	Nanocrystalline, Iron-based Alloy, Cobalt-based Alloy and Ferrite (Mn-Zn)
Temperature constraint	Temperature rise: 60 [°C], Ambient temperature: 40 [°C]
Winding design	Maximum number of layer: 10. Maximum conductor diameter: 12 [mm]

Table 2: Specification of topology example

(a) Power Losses

(b) Volume

Figure 5: Power losses and Volume for RMC with single-phase Transformer
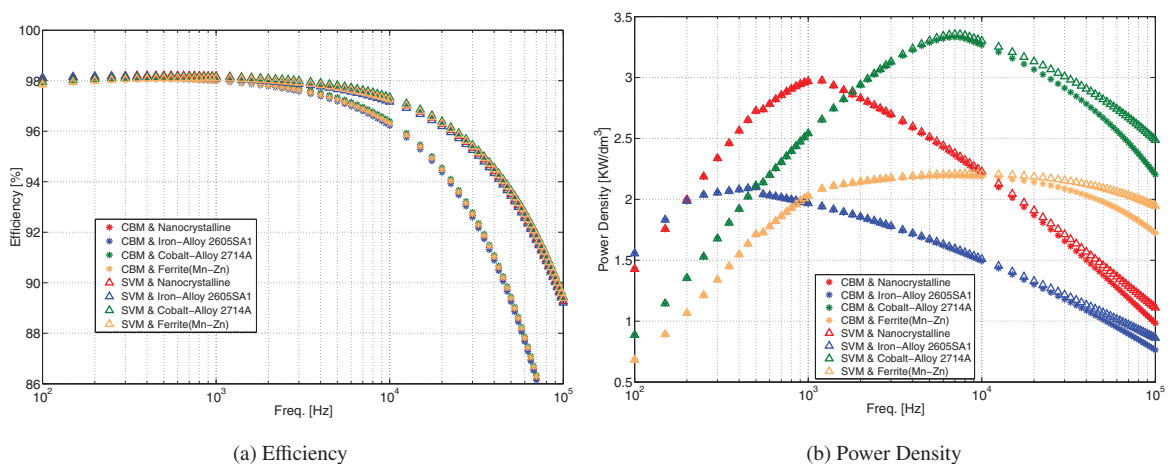

(a) Efficiency

(b) Power Density

Figure 6: Efficiency and Power Density for RMC with single-phase Transformer
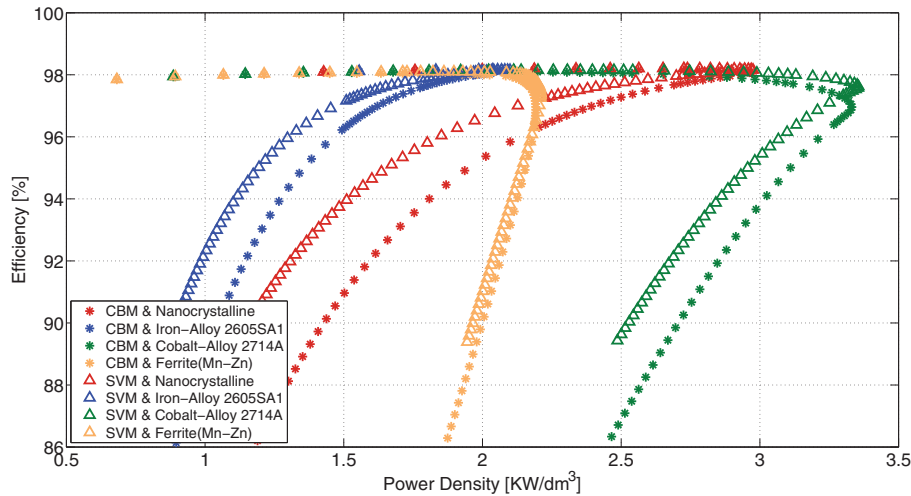
Figure 7: Pareto-Front: Efficiency Power-Density

for simplicity that the turn ratio is 1:1. Four core materials are taken into account: nanocrystalline material (FINEMET), Iron-based amorphous alloy 2605SA1 (POWERLITE), Cobalt-based amorphous alloy 2714A (MAGNAPERM) and Ferrite (Mn - Zn). The Ferrite parameters are reported in [6], the others core parameters are taken from the data sheet manufacturer (Metglas®).

In Fig. 5 shows the total power losses and volume at different frequencies. From Fig. 5a, it is clear that the total loss depend on the switching frequency. Also, the modulation scheme has a significant effect on losses and becomes more notable as the switching frequency increases. The SVM scheme has lower losses as it is reported in [3]. On the other hand, the volume obtained in the design process depends greatly on the frequency and the selected core material as can be seen in Fig. 5b. For the selected core materials can highlight two options: Nanocrystalline for frequencies near 1 [kHz], and Cobalt-based amorphous alloy 2714A for frequencies around 10 [kHz].

The evaluation of efficiency and power density for the considered topology are presented in Fig. 6. System efficiency decreases as the frequency increases, as shown in Fig. 6a. Also, it can be noted that the modulation scheme has a greater impact on efficiency than the core material, which can be deduced from the analysis of losses in Fig. 5a. On the other hand, the type of core material influences the maximum power-density value and the frequency at which this value is obtained, as shown in Fig. 6b. Again, Cobalt-based amorphous alloy material presents a better choice for frequencies above 2 [KHz] and nanocrystalline material for frequencies around 1 [kHz]. Also, it can be observed that the power-density is more affected by the modulation scheme at high frequencies than at low frequencies.

Finally, the Pareto front of efficiency and power density can be plotted. Fig. 7 shows the Pareto front of RMC and single-phase transformer for the set of parameters considered.

4. Conclusion

A simple procedure for evaluation of efficiency and power density of power conversion topologies for wind turbines has been described. The model takes account of two main components of the converter system, the power electronics devices and the high frequency transformer. The evaluation of efficiency and power density has been related to calculate the total power losses and the volume of the system. Accurate approximations have been provided to facilitate the evaluation of the losses and volume. The proposed procedure has been illustrated with the reduced matrix converter and single-phase transformer topology. The methodology is eminently suitable for comparison of power converter with different topologies.

Acknowledgements

References

[1] M. Liserre, R. Cardenas, M. Molinas, J. Rodriguez, Overview of Multi-MW wind turbines and wind parks, IEEE Transactions on Industrial Electronics 58 (4) (2011) 1081–1095. doi:10.1109/TIE.2010.2103910.

[2] J. W. Kolar, J. Biela, S. Waffler, T. Friedli, U. Badstuebner, Performance trends and limitations of power electronic systems, in: 2010 6th International Conference on Integrated Power Electronics Systems (CIPS), IEEE, 2010, pp. 1–20.

[3] A. Garces, M. Molinas, Comparative investigation of losses in a reduced matrix converter for off-shore wind turbines, in: 5th IET International Conference on Power Electronics, Machines and Drives (PEMD 2010), IET, 2010, pp. 1–6. doi:10.1049/cp.2010.0096.

[4] M. R. Hanssen, A. G. Ruiz, M. Molinas, Operation features of a reduced matrix converter for offshore wind power, in: 2010 IEEE International Symposium on Industrial Electronics (ISIE), IEEE, 2010, pp. 2443–2448. doi:10.1109/ISIE.2010.5637732.

[5] A. Odaka, J. Itoh, I. Sato, H. Ohguchi, H. Kodachi, N. Eguchi, H. Umida, Analysis of loss and junction temperature in power semiconductors of the matrix converter using simple simulation methods, in: Conference Record of the 2004 IEEE Industry Applications Conference, 2004. 39th IAS Annual Meeting, Vol. 2, IEEE, 2004, pp. 850– 855 vol.2. doi:10.1109/IAS.2004.1348512.

[6] W. G. Hurley, W. H. Wolfle, J. G. Breslin, Optimized transformer design: inclusive of high-frequency effects, IEEE Transactions on Power Electronics 13 (4) (1998) 651–659. doi:10.1109/63.704133.

[7] H. R. Karampoorian, G. Papi, A. Zadehgol, Volume and loss optimization of high frequency transformer for compact switch mode power supply considering corrected waveform factor, in: 2006 IEEE Power India Conference, IEEE, 2006. doi:10.1109/POWERI.2006.1632487.

[8] W. Shen, F. Wang, D. Boroyevich, C. W. Tipton, Loss characterization and calculation of nanocrystalline cores for High-Frequency magnetics applications, IEEE Transactions on Power Electronics 23 (1) (2008) 475–484. doi:10.1109/TPEL.2007.911881.

[9] P. L. Dowell, Effects of eddy currents in transformer windings, Proceedings of the Institution of Electrical Engineers 113 (8) (1966) 1387–1394. doi:10.1049/piee.1966.0236.

[10] N. Mohan, T. M. Undeland, W. P. Robbins, Power Electronics: Converters, Applications, and Design, 3rd Edition, Wiley, 2002.

[11] R. A. Jabr, Application of geometric programming to transformer design, IEEE Transactions on Magnetics 41 (11) (2005) 4261–4269. doi:10.1109/TMAG.2005.856921.

[12] W. G. Hurley, Optimizing core and winding design in high frequency transformers, in: Power Electronics Congress, 1996. Technical Proceedings. CIEP '96., V IEEE International, IEEE, 1996, pp. 2–13. doi:10.1109/CIEP.1996.618452.

[13] A. Garces, M. Molinas, A study of efficiency in a reduced matrix converter for offshore wind farms, IEEE Transactions on Industrial Electronics 59 (1) (2012) 184–193. doi:10.1109/TIE.2011.2130502.

[14] A. Garces, M. Molinas, Impact of operation principle on the losses of a reduced matrix converter for offshore wind parks, in: 2010 IEEE International Symposium on Industrial Electronics (ISIE), IEEE, 2010, pp. 2412–2419. doi:10.1109/ISIE.2010.5637529.

[15] A. Garces, M. Molinas, Reduced matrix converter operated as current source for off-shore wind farms, in: Power Electronics and Motion Control Conference (EPE/PEMC), 2010 14th International, IEEE, 2010, pp. T12–149–T12–154. doi:10.1109/EPEPEMC.2010.5606549.

[16] A. Garces, M. Molinas, Electrical conversion system for offshore wind turbines based on high frequency ac link, in: IX International Conference and Exhibition of Renewal Energy and Ecological Vehicles EVER2009, Monaco, 2009.